

## Technical note

## A new method for processing of continuous intracranial pressure signals

Per Kristian Eide\*

*Department of Neurosurgery, The National Hospital (Rikshospitalet), 0027 Oslo, Norway*

Received 13 March 2005; received in revised form 25 July 2005; accepted 28 September 2005

**Abstract**

This paper describes a new method for processing of continuous pressure signals. Continuous intracranial pressure (ICP) signals were sampled at 100 Hz, converted into digital data and processed during 6 s time windows. According to a new algorithm, cardiac beat-induced single ICP waves were identified; pressure waves caused by noise in the signal were rejected for further analysis. The amplitude and latency values of the accepted single ICP waves were determined. For accepted 6 s time windows, the mean ICP wave was computed as mean ICP wave amplitude and mean ICP wave latency. Mean ICP for every time window was computed according to current practice as sum of pressure levels divided by number of samples. The mean ICP wave parameters provide information about the single ICP waves that is not given by mean ICP. The method has been implemented in software to be used during online ICP monitoring, revealing mean ICP wave amplitude, mean ICP wave latency and mean ICP as numerical values every 6 s. The values are presented in trend plots. Verification of correct single ICP wave identification can be done during online ICP monitoring. The clinical significance of the method was illustrated in four patients by observations that mean wave amplitudes corresponded better to the acute clinical state than the mean ICP; mean wave amplitudes could be elevated despite a normal mean ICP. In one patient with ICP and arterial blood pressure (ABP) signals monitored simultaneously with identical time reference, there was a weak correlation between mean ICP and ABP wave amplitudes. It is tentatively suggested that the mean ICP wave parameters are related to intracranial pressure–volume compensatory reserve capacity (compliance).

© 2005 IPPEM. Published by Elsevier Ltd. All rights reserved.

**Keywords:** Intracranial pressure; Single pressure waves; ICP analysis**1. Introduction**

Continuous intracranial pressure (ICP) monitoring has been found helpful in handling patients with, e.g. head injury, stroke and hydrocephalus [1–3]. According to current guidelines mean ICP should be kept below 15–20 mmHg to prevent secondary cerebral ischemia and to maintain adequate intracranial compensatory reserve capacity (compliance) [1–3]. Intracranial compliance refers to the relationship between intracranial pressure change and volume change, as expressed in the pressure–volume curve [4–8]. During reduced intracranial compliance, a small increase in the intracranial volume produces large increases in mean ICP.

Current state-of-art technology computes mean ICP during short time windows (e.g. 5–15 s duration) without considering the single ICP waves created by the cardiac contractions. This may impose a limitation regarding ICP monitoring since single ICP wave amplitudes (pulse pressure) probably more reliably predict intracranial compliance than mean ICP alone [1–3]. Pulse pressure increased when intracranial compliance was reduced [4,9]; and a linear relationship existed between mean ICP and pulse pressure when mean ICP was below 30–60 mmHg [4,9–13]. According to the hydrodynamic theories, it has been suggested that reduced intracranial compliance is an important mechanism behind communicating hydrocephalus [14]. Hence, pulse pressure was a better predictor of hydrocephalus than mean ICP alone [15,16].

More recently information about single ICP waves has been derived from spectral analysis using fast Fourier transformation (FFT) [10,17–21]. However, FFT does not include

\* Tel.: +47 23074300; fax: +47 23074310.

E-mail address: [per.kristian.eide@rikshospitalet.no](mailto:per.kristian.eide@rikshospitalet.no).

an algorithm for identification of the single ICP waves. Information about single ICP waves derived from FFT depends on the quality of ICP signals, e.g. related to sudden variations in pressures and heart rate.

Nevertheless, mean ICP remains the information used in current clinical practice during continuous ICP monitoring. The author previously developed methods for quantitative analysis of mean ICP levels, although these methods did not include single ICP wave analysis [22,23]. In order to obtain information about intracranial compliance by single ICP wave analysis, the author developed a new method for processing continuous ICP signals that is described in this paper. In short, for every 6 s time window of a continuous ICP signal, the mean ICP wave is computed as mean ICP wave amplitude and mean ICP wave latency. These two single ICP wave parameters can be presented online as numerical values during continuous ICP monitoring, thus providing information about single ICP waves. In addition, mean ICP for every 6 s time window is computed according to current practice to compare against state-of-art technology.

## 2. Materials and methods

### 2.1. Monitoring of continuous ICP signals

The procedure of the continuous ICP monitoring is briefly described. Following calibration against atmospheric pressure, a solid ICP sensor (Codman MicroSensor™, Johnson & Johnson, Raynham, MA, USA) was introduced 1–2 cm into the frontal brain parenchyma through a minimal opening in the dura, and coupled to a Codman® pressure transducer (Codman ICP Express™, Johnson & Johnson, Raynham), which again was coupled to a vital signs Siemens 9000 XL Series Monitor (Siemens Medical Systems Inc., Danvers, MA, USA). By means of the Siemens Infinity Gateway Software (Siemens Medical Systems Inc., Danvers), the continuous ICP signals were transferred online via the hospital network to a computer server and stored as raw data files (sampling rate 100 Hz).

The software SM NeuroWave Version 2.0 (Sensometrics AS, Oslo, Norway) was used to further analyze the continuous ICP signals. The method implemented in this software is further detailed in Sections 2.2 and 2.3.

The first part of the signal conditioning is the software filter; a 25th order Bessel low pass filter, with a 25 Hz cut-off frequency was used. This is an ordinary filtering procedure.

### 2.2. Processing of continuous ICP signals

An overview of the method for processing of continuous ICP signals is shown in Fig. 1. The algorithm is composed of three main steps: (i) localization of single pressure waves; (ii) extraction of features from each single pressure wave and (iii) determination of average of parameters on 6 s time windows.

First, all peaks and valleys in the sampled ICP signal are identified. Each peak and valley is a sample with a pressure value and a time stamp or location. According to *General Methods Criteria*, pair combinations of peaks and valleys in the signal are identified: all peaks and valleys within two subsequent time windows are identified, their absolute pressure values are determined, and the percentage of peaks and valleys with given absolute pressure values are determined. The peaks and valleys with absolute pressure values within the majority pressure range of the two subsequent time windows are identified. The peak and valley detection uses an algorithm that fits a quadratic polynomial to sequential groups of data points. The width parameter specifies the number of consecutive data points to use, wherein 10 are used during a sampling rate of 100 Hz and 20 during a sampling rate of 200 Hz. For each peak or valley, the function tests the quadratic fit against the threshold parameters; the threshold within a specified time window is set to maximum sample value during valley detection or minimum sample value during peak detection.

Second, a moving time window of 0.1 s is used to select nearby peaks or valleys for further analysis. When several peaks are identified within a moving time window of 0.1 s, only the peak with greatest absolute pressure value is selected. When several valleys are identified within a moving time window of 0.1 s only the valley with the lowest absolute pressure value is selected. Third, there cannot be two peak/valley pair combinations within a single ICP wave duration. Fourth, two different pair peak/valley combinations cannot contain identical peaks or valleys. Locations of peaks and valleys within a recording are all unique since location is unique for each sample value. Hence, it is required that there cannot be two valleys with the same location or one peak with the same location as a valley. The output is accepted peak/valley pairs. For accepted peak/valley pairs, the single wave amplitude (SW.dP) and latency (SW.dT) values are determined.

According to *Single Wave Criteria*, single ICP wave amplitude (SW.dP) should be between 1.0 and 35.0 mmHg and single ICP wave latency (SW.dT) between 0.08 and 0.40 s. The choice of these thresholds was based on a systematic testing how different thresholds affected single wave detection. In a prototype of the software thresholds could be changed, and single wave detection studied in the raw ICP signal. Since the pressure recordings are stored as raw data files, it is possible to examine how different thresholds affect single wave detection. To this end a large number of continuous ICP recordings have been tested; through a visual inspection of these ICP recordings it has been verified how the criteria differentiate between artifacts and the single ICP waves. The output is a number of accepted single ICP waves during a 6 s time window of the signal. A 6 s time window refers to a selected time frame of the pressure-related digital data with a time reference.

According to *Time Sequence Criteria*, the numbers of single pressure waves within a time window should be between

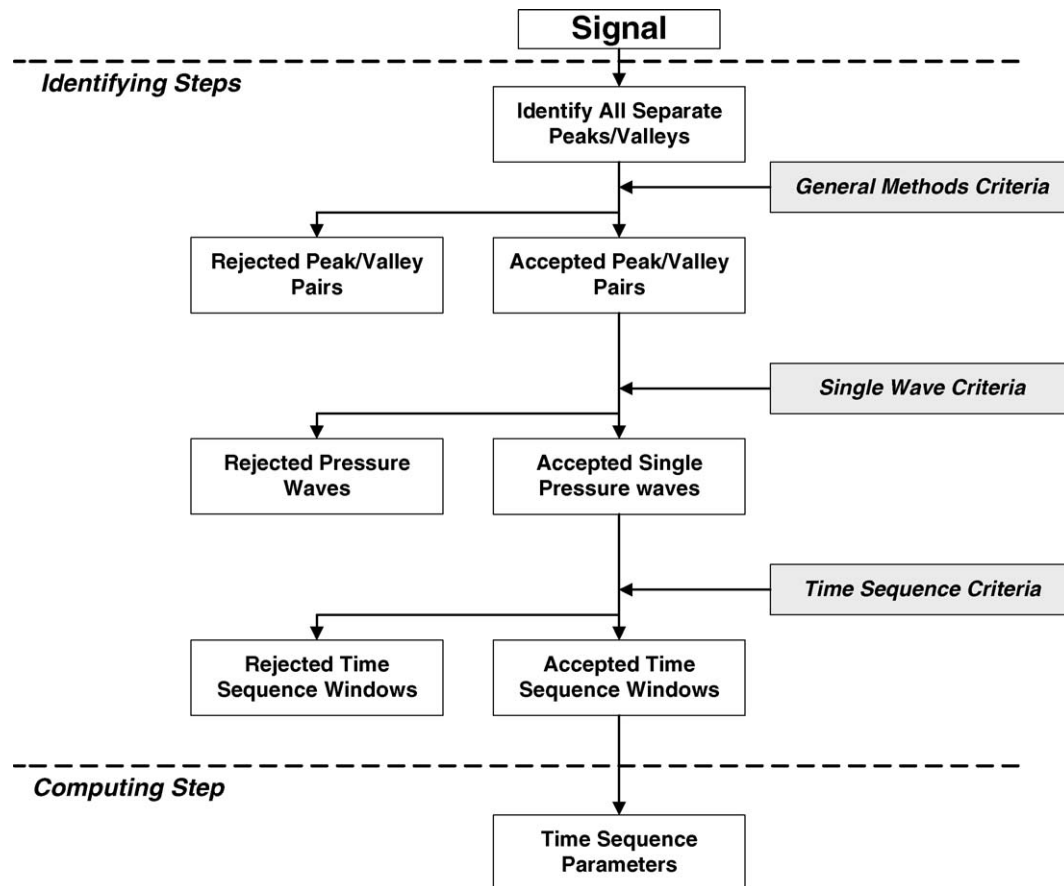


Fig. 1. The algorithm of processing continuous ICP signals includes Identifying and Computing Steps resulting in determination of mean ICP, mean ICP wave amplitude and mean ICP wave latency during 6 s time windows (time sequence parameters).

4 and 18 (corresponding to a heart rate of  $40\text{--}180\text{ min}^{-1}$ ). Furthermore, a first single ICP wave within a time window must have its ending diastolic minimum pressure value within this time window; and a last single ICP wave within a time window must have both its starting and ending diastolic minimum pressure values within the time window.

The algorithm is illustrated in Fig. 2a and b. In Fig. 2a is shown all 22 identified peaks (filled squares) and all 17 identified valleys (open circles). In Fig. 2b is shown the accepted peak/valley pair combinations of systolic maximum pressure ( $\text{SW}[6].P_{\max}$ ) and starting diastolic minimum pressure ( $\text{SW}[6].P_{\min1}$ ), characterizing single ICP waves created by the cardiac beat-induced pressure waves.

The single ICP wave parameters of single wave 6 ( $\text{SW}[6]$ ) of the time window shown in Fig. 2b are illustrated in Fig. 2c. The starting diastolic minimum pressure of the single wave ( $\text{SW}[6].P_{\min1}$ ) defines the start of the single wave, the ending diastolic minimum pressure ( $\text{SW}[6].P_{\min2}$ ) defines the end of the single wave, and the systolic maximum pressure ( $\text{SW}[6].P_{\max}$ ) defines the maximum of the single wave. Single wave amplitude ( $\text{SW}[6].dP$ ) is the pressure difference when pressures increase from starting diastolic minimum pressure to systolic maximum pressure; single wave latency ( $\text{SW}[6].dT$ ) is the time interval when the pressures change

from starting diastolic minimum pressure to systolic maximum pressure. Wave duration ( $\text{SW}[6].WD$ ) is the time duration between starting diastolic minimum pressure and ending diastolic minimum pressure of the single ICP wave.

For accepted time windows, the three parameters mean ICP, mean ICP wave amplitude and mean ICP wave latency are computed in the Computing Step (Fig. 1).

Mean ICP represents current state-of-art technology, computed as the sum of all pressure sample levels divided by the numbers of samples. For the time window shown in Fig. 2b, mean ICP was 11.65 mmHg (i.e. the sum of pressure levels of 6989.4 mmHg were divided by the number of samples of 600 that correspond to a sampling rate of 100 Hz during 6 s).

The procedure of computing mean ICP wave amplitude and mean ICP wave latency is described with reference to the accepted single ICP waves shown in Fig. 2b. A matrix is created (Table 1); one axis being related to an array of pre-selected values of single ICP wave amplitude ( $\text{SW}.dP$ ) and another axis being related to an array of pre-selected values of single ICP wave latency ( $\text{SW}.dT$ ). For each matrix cell at respective intersections is indicated a number of occurrences of matches between specific single ICP wave amplitude and latency values. A small part of such a matrix of 1800 cells is presented in Table 1, illustrating the occurrence

Table 1

The occurrence of single ICP wave amplitude (dP) and latency (dT) combinations during the time window shown in Fig. 2b

Group name		0.5	1	1.5	2	2.5	3	3.5
Group range		0.5 ≤ dP < 1.0	1.0 ≤ dP < 1.5	1.5 ≤ dP < 2.0	2.0 ≤ dP < 2.5	2.5 ≤ dP < 3.0	3.0 ≤ dP < 3.5	3.5 ≤ dP < 4.0
Group midpoint		0.75	1.25	1.75	2.25	2.75	3.25	3.75
0.1	0.10 ≤ dT < 0.11	0.105				1	1	
0.11	0.11 ≤ dT < 0.12	0.115					1	
0.12	0.12 ≤ dT < 0.13	0.125						
0.13	0.13 ≤ dT < 0.14	0.135						
0.14	0.14 ≤ dT < 0.15	0.145						
0.15	0.15 ≤ dT < 0.16	0.155						
0.16	0.16 ≤ dT < 0.17	0.165						
0.17	0.17 ≤ dT < 0.18	0.175						
0.18	0.18 ≤ dT < 0.19	0.185						
0.19	0.19 ≤ dT < 0.20	0.195						
0.2	0.20 ≤ dT < 0.21	0.205					1	
0.21	0.21 ≤ dT < 0.22	0.215						
0.22	0.22 ≤ dT < 0.23	0.225						
0.23	0.23 ≤ dT < 0.24	0.235						1
0.24	0.24 ≤ dT < 0.25	0.245				1		
0.25	0.25 ≤ dT < 0.26	0.255						
0.26	0.26 ≤ dT < 0.27	0.265					1	
0.27	0.27 ≤ dT < 0.28	0.275						
0.28	0.28 ≤ dT < 0.29	0.285						

of SW.dP/SW.dT combinations of the seven single pressure waves (SW[1] to SW[7]) shown in Fig. 2b.

The method comprises the further step of computing balanced position of the occurrence of SW.dP/SW.dT combinations, which corresponds to mean wave amplitude and mean wave latency. First, the latency (SW.dT) mean value (or row mean), with respect to the amplitude (SW.dP) values (columns) is determined ( $m_i$ ). The  $m_i$  for each row is determined by using the Eq. (1).

$$m_i = \sum_{j=1}^c A_j w_{ij} \quad (1)$$

$A_j$  is the  $j$ th column midpoint, referring to an amplitude (SW.dP) group value and  $w_{ij}$  the frequency (count) of the  $i$ th SW.dT row and  $j$ th SW.dP column cells.

$$\text{Row mean} = \text{Mean}(dT) = \frac{\sum_{i=1}^r m_i B_i}{\sum_{i=1}^r m_i} \quad (2)$$

$B_i$  is the  $i$ th row SW.dT midpoint value ( $r$  = row). The terms “ $i$ th SW.dT row and  $j$ th SW.dP column cell” refer to a matrix cell with the coordinates “ $i$ th row and  $j$ th column cell”. As further detailed in Table 2, using the Eqs. (1) and (2) gives a row mean with respect to columns of 0.184 s (4.086/22.25).

Second, the mean (SW.dP) value (columns), with respect to the latency (SW.dT) value (rows), is determined ( $m_j$ ). The  $m_j$  for each SW.dP column is found, as given in Eq. (3).

$$m_j = \sum_{i=1}^r B_i w_{ij} \quad (3)$$

Table 2

Computation of row (latency) mean with respect to columns (amplitude)

$m_i$	SW.dT <sub>i</sub>	$m_i \times \text{SW.dT}_i$
$(1 \times 2.75) + (1 \times 3.25) = 6.0$	0.105	0.630
$1 \times 3.25 = 3.25$	0.115	0.374
$1 \times 3.25 = 3.25$	0.205	0.666
$1 \times 3.75 = 3.75$	0.235	0.881
$1 \times 2.75 = 2.75$	0.245	0.674
$1 \times 3.25 = 3.25$	0.265	0.861
Sum = 22.25		4.086
Row mean: 4.086/22.25 = 0.184 s		

$B_i$  is the  $i$ th row SW.dT midpoint, referring to a SW.dT group value and  $w_{ij}$  is the frequency for the  $i$ th row and  $j$ th column.

$$\text{Column mean} = \text{Mean}(dP) = \frac{\sum_{j=1}^c m_j A_j}{\sum_{j=1}^c m_j} \quad (4)$$

$A_j$  is the  $j$ th column SW.dP value midpoint ( $c$  = column). The calculations are shown in Table 3, using the Eqs. (3) and (4), the column mean with respect to rows will be equal to 3.205 mmHg (4.087/1.275).

Table 3

Computation of column (amplitude) mean with respect to rows (latency)

$m_j$	SW.dP <sub>j</sub>	$m_j \times \text{SW.dP}_j$
$(1 \times 0.105) + (1 \times 0.245) = 0.35$	2.75	0.963
$(1 \times 0.105) + (1 \times 0.115) + (1 \times 0.205) + (1 \times 0.265) = 0.690$	3.25	2.243
$1 \times 0.235 = 0.235$	3.75	0.881
Sum = 1.275		4.087
Column mean: 4.087/1.275 = 3.205 mmHg		

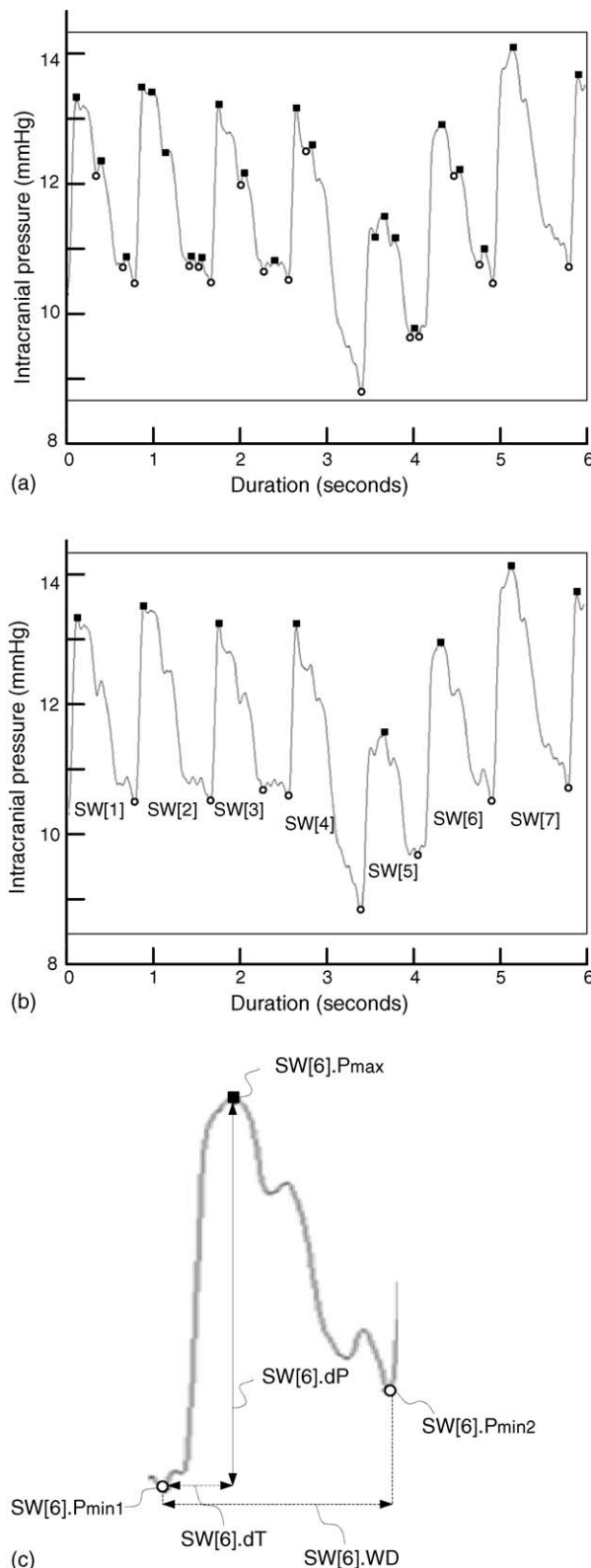


Fig. 2. One 6 s time window is shown with (a) all identified peaks (maximum pressure values) and valleys (minimum pressure values), and (b) only the accepted peak/valley pairs. Among the accepted single ICP waves (SW[1] to SW[7]) of this time window, it is shown (c) the features of single wave six (SW[6]).

Thus, the mean ICP wave of the time window in Fig. 2b had mean wave amplitude of 3.33 mmHg and mean wave latency of 0.17 s.

### 2.3. Processing of continuous ABP signals

One of the patients had raw signals of simultaneous continuous ICP and ABP recordings with identical time reference. The continuous ABP signal was derived from a cannula placed within the radial artery and connected to a Baxter Truwave PX-600F vein/arterial anesthesia pressure monitoring kit (Baxter Healthcare, Chicago, USA). Processing of continuous ABP signals was performed as described for ICP signals described in Section 2.2. Concerning *Single Wave Criteria*, single ABP wave amplitude should be between 20 and 150 mmHg and single ABP wave latency between 0.10 and 0.40 s. Mean ABP wave amplitudes were computed with the same method as the mean ICP wave amplitudes, except from the threshold values. In order to investigate a possible relationship between mean ICP and ABP wave amplitudes, the trend plots of mean ICP and ABP wave amplitudes were compared (Fig. 4a). Furthermore, all the 6000 corresponding mean ICP and ABP wave amplitude values shown in the trend plot were plotted in a scatter plot including the regression line (Fig. 4b). The Pearson's correlation coefficient was computed.

A single wave match test incorporating both a visual inspection of matched ICP and ABP single waves and determination of a percent hit rate showed that the single ICP waves appear 0.01–0.03 s before the single ABP waves with our measuring equipment.

### 2.4. Patients

The continuous ICP recordings of four individuals were presented to illustrate the new method. Cases A and B (both 10 years of age) underwent ICP monitoring to assess hydrocephalus-related intracranial hypertension, including headache, lethargy and radiological ventricular enlargement. Case C was a 59 years old woman intubated and sedated on the respirator, undergoing continuous ICP and ABP monitoring due to severe subarachnoid and parenchyma hemorrhage. Case D was a 65 years old woman undergoing intracranial monitoring due to suspected normal pressure hydrocephalus with radiological enlargement of cerebral ventricles and severe symptoms (complete dependency, inability to stand up, urinary incontinence and severe dementia).

### 2.5. Statistics

Determination of Pearson's correlation coefficient was performed in SPSS, Version 12.0 (SPSS Inc., Chicago, IL).

## 3. Results

In order to verify the algorithm, the continuous ICP signals were visually inspected for correct peak/valley pair detec-



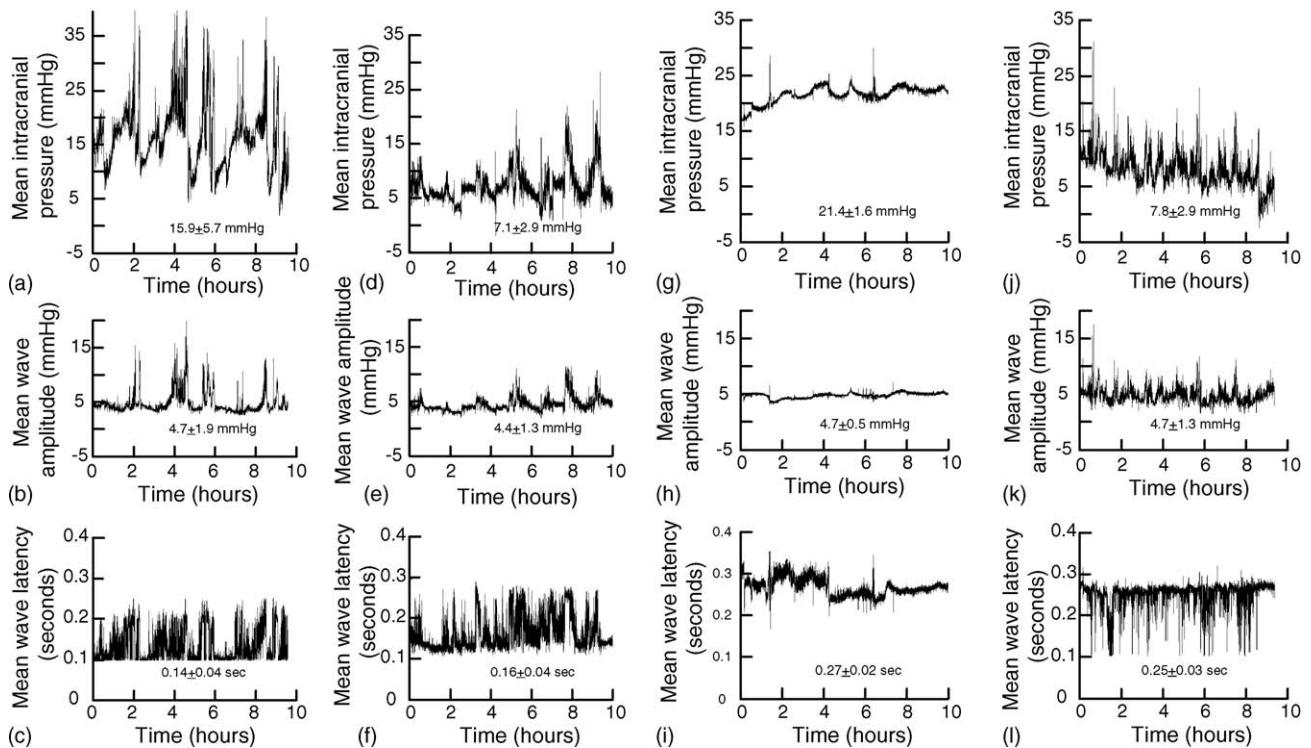


Fig. 3. The continuous ICP recordings of Cases A (a–c), B (d–f), C (g–i) and D (j–l) are presented as trend plots of mean ICP (a, d, g, j), mean ICP wave amplitude (b, e, h, k) and mean ICP wave latency (c, f, i, l) computed every consecutive 6 s time window. The mean value  $\pm$  standard deviation of each trend plot is shown.

tions. This is illustrated in Fig. 2b, as peak/valley pairs of the seven accepted single pressure waves during a 6 s time window. In Case C with simultaneous continuous ICP and ABP signals with identical time reference, visual inspection of the raw signals showed that single ICP and ABP waves corresponded. The percentage of corresponding single ICP and ABP waves were computed automatically. With regard to the recording of Case C, 97% of the single ICP waves were corresponding to the ABP waves. The percentage increased to above 99% when excluding periods with artifacts within the ABP and/or ICP signals. Hence, the percentage of artifact-induced pressure waves misinterpreted as single ICP waves by this algorithm is low.

For the continuous ICP recordings shown in Fig. 3, the numbers of accepted and rejected time windows were computed; the numbers of accepted time windows were 5748 for Case A (Fig. 3a–c), 5999 for Case B (Fig. 3d–f), and 6000 for Case C (Fig. 3g–i) and 5594 for Case D (Fig. 3j–l). Each of these ICP recordings lasted 10 h and included 6000 time windows each. For these four recordings the percentage of rejected time windows ranged between 0 and 6.8%. Thus, the percentage of time windows rejected by the algorithm is rather low.

The pressure recordings of Case A (Fig. 3a–c) and Case B (Fig. 3d–f) showed very different mean ICP values, though mean wave amplitude and mean wave latency were comparable. In these two cases the clinical picture was comparable;

the clinic was best related to the mean wave amplitude and latency values.

The pressure recordings of Case C (Fig. 3g–i) and Case D (Fig. 3j–l) also showed marked differences in mean ICP, though mean wave amplitude and mean wave latency were comparable. Case C was critically ill and died after 11 days in the intensive care unit. Case D, on the other hand, showed a remarkable clinical improvement after implantation of an extra-cranial shunt draining cerebrospinal fluid. The patient became able to walk independently, urinary continent and being able to communicate properly. In this latter case mean wave amplitudes were abnormally high despite a normal mean ICP.

In Fig. 4a is shown the trend plots of mean wave amplitude derived from the simultaneous ICP (lower curve) and ABP (upper curve) signals of Case C, and in Fig. 4b is shown a scatter plot of the 6000 corresponding mean ICP and ABP wave amplitudes including the regression line. A Pearson's correlation coefficient of 0.33 was computed ( $P < 0.001$ ).

#### 4. Discussion

This paper describes a method of computing the mean ICP wave (mean ICP wave amplitude and latency) within a time window. A crucial task of the algorithm is to identify the single ICP waves created by the cardiac contractions.

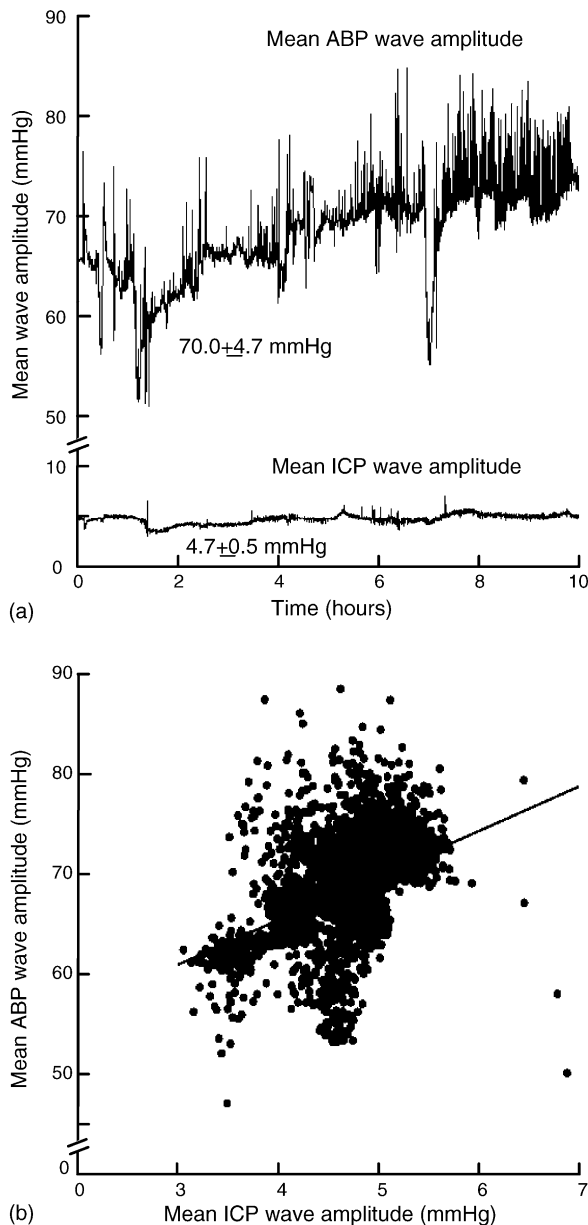


Fig. 4. The 10 h continuous ICP/ABP recording of Case C is presented as (a) trend plots of 6000 mean ICP wave amplitude values (lower curve) and 6000 mean ABP wave amplitude values (upper curve). The mean value  $\pm$  standard deviation of each trend plot is shown. The correlation between the 6000 corresponding mean ICP and ABP wave amplitude values is indicated in (b) a scatter plot, including the regression line. The Pearson's correlation coefficient was 0.33.

This may not be straightforward since biological signals are dynamic; hence the pressure signals often contain pressure waves related to noise in the signal. The algorithm has been tested on-line on numerous continuous ICP signals. By visual inspection of the waveform it has been verified that accepted peak/valley pairs correspond to systolic maximum pressure ( $SW.P_{max}$ ) and starting diastolic minimum pressure

( $SW.P_{min1}$ ) values of the single ICP waves. Since the continuous ICP recordings are stored as raw data ICP files, it has as well been verified off-line that the algorithm performs correct peak/valley detections. Moreover, simultaneous continuous ICP and ABP recordings with identical time reference have made it possible to verify that single ICP and ABP waves correspond. Within the pressure recording of Case C, only 3% of single ICP waves did not correspond to the single ABP waves, which was partly due to artifacts within the ABP signal itself. To this end the author has applied the algorithm on a large number of continuous ICP and ABP recordings, thus providing evidence that the algorithm differentiate between cardiac beat-induced single ICP waves and pressure waves caused by noise in the ICP signal.

Previously mean ICP and pulse pressures were examined by visual inspection of pressure charts, wherein pulse pressure was the pressure difference between systolic maximum and diastolic minimum pressures [4,9,11,16]. Computer-assisted determinations of pulse pressure as difference between systolic maximum and diastolic minimum pressures have been reported, although without criteria for correct systolic maximum and diastolic minimum pressure detections [13,24]. On the other hand, analyzing single ICP waves by spectral analysis using FFT [10,17–21] does not include identification of single ICP wave systolic maximum or diastolic minimum pressure values.

It was selected to process signals within 6 s time windows since most modern vital signs monitors/pressure transducers update the calculated pressure values each 5–10 s. In pilot tests it was found that analysis results were similar whether time window durations were 5 or 8 s. Others have performed ICP analysis during time windows lasting from a few seconds to several minutes and even hours [18,19,21].

When it was required that accepted 6 s time windows should contain 4–18 single ICP waves, this requirement corresponds to a heart rate of 40–180 beats/min. Heart rates outside these ranges might give problems regarding single ICP wave identification.

Since a continuous pressure signal contains two dimensions (pressure and time scales), every peak and valley have a pressure value and a time stamp or location. Hence, every single ICP wave (Fig. 2c) should be described in both dimensions; and both dimensions should be considered when computing the mean ICP wave within a time window. Preliminary results suggested that both the amplitude and latency values have a physiological role; both single wave amplitude and latency values increased with increasing mean ICP values. In order to consider both the amplitude and latency values, a two-dimensional matrix of single wave amplitude (columns) and latency (rows) groups. Thus, the mean column ( $SW.dP$ ) value must be computed with respect to the row ( $SW.dT$ ) value and vice versa. Thereby, both dimensions of the single ICP wave are considered when computing the mean wave of a time window.

To this end we have observed mean ICP wave amplitudes between 1 and 35 mmHg and mean ICP wave latencies

between 0.08 and 0.40 s. This was the reason for including a rather large number of single wave amplitude and latency groups in the two-dimensional matrix (Table 1). For amplitude groups increments of 0.5 mmHg were used and for latency groups increments of 0.01 s. Obviously, other increment levels could as well be used, but these levels were found useful from a clinical point of view. It was selected to use a fixed matrix for ICP signals to make comparisons between matrix distributions easier.

Mean ICP is computed relative to the atmospheric pressure as the difference between the pressure within the intracranial compartment and the atmospheric pressure. For several ICP sensors including the Codman MicroSensor used in the present patients, calibration against atmospheric pressure is only performed during sensor implantation. Therefore, mean ICP values are dependent on zero pressure level as well as sensor drift. The mean ICP wave parameters, on the other hand, refer to relative differences in pressure (mean wave amplitude) and time (mean wave latency), which are independent on zero pressure level and drift.

The continuous ICP recordings of four patients were presented in this paper to illustrate the clinical significance of the new algorithm. The clinical pictures of patients A and B corresponded better to mean ICP wave amplitude and latency values than to mean ICP. In patients C and D mean ICP differed considerably despite comparable mean wave amplitude and latency values. In Case D with normal pressure hydrocephalus mean ICP wave amplitude and latency values were abnormally increased though mean ICP was normal. This patient responded clinically very markedly to reduction of mean ICP wave amplitudes and latency values by extracranial shunt treatment. Thus, in these four cases the mean ICP wave parameters provided information not revealed by mean ICP.

It may tentatively be suggested that mean ICP wave amplitude and latency are related to intracranial compliance (pressure–volume compensatory reserve capacity). The single ICP wave amplitude can be considered as the pressure response to every cardiac beat-induced pressure wave [4,9], although the intracranial blood volume change caused by each cardiac contraction cannot be determined. Other complicating factors are that every single ICP wave is a complex function of the arterial and venous hemodynamic variables as well as other intracranial variables such as the cerebral vasomotor tone [20,25–28].

Though the single ICP waves are created from the cardiac contractions, another question is whether the ICP pulse pressure is directly related to the ABP pulse pressure [19,20,27–29]. Patient C had both her ICP and ABP monitored. Since both signals were simultaneous with identical time reference, the Pearson's correlation coefficient could be determined between mean ICP wave amplitude and mean ABP wave amplitude. Given a good correlation the Pearson's correlation coefficient should be close to 1. However, as indicated in Fig. 4b, the correlation coefficient was 0.3. The correlation was significant due to a very large number

of 6000 corresponding values in the plot. Nevertheless, in this patient there was a weak correlation between mean wave amplitudes of corresponding single ICP and ABP signals. Similar observations have been made in other patients.

## 5. Conclusions

This paper describes an algorithm for computing the mean ICP wave (mean ICP wave amplitude and latency) within 6 s time windows of a continuous ICP signal. In addition mean ICP is computed according to current practice. The mean ICP wave parameters provide information about single ICP waves not given by mean ICP. It is tentatively suggested that the mean ICP wave parameters are more useful for prediction of intracranial compliance than mean ICP alone.

## References

- [1] Czosnyka M, Pickard JD. Monitoring and interpretation of intracranial pressure. *J Neurol Neurosurg Psychiatry* 2004;75:813–21.
- [2] Doyle DJ, Mark PWS. Analysis of intracranial pressure. *J Clin Monitor* 1992;8:81–90.
- [3] Lee KR, Hoff JT. Raised intracranial pressure and its effect on brain function. In: Crockard A, Hayward R, Hoff JT, editors. *Neurosurgery. The scientific basis of clinical practice*. Blackell Science; 2000. p. 393–409.
- [4] Avezaat CJJ, van Eijndhoven JHM, Wyper DJ. Cerebrospinal fluid pulse pressure and intracranial volume-pressure relationships. *J Neurol Neurosurg Psychiatry* 1979;42:687–700.
- [5] Langfitt TW, Weinstein JD, Kassell NF. Cerebral vasomotor paralysis produced by intracranial hypertension. *Neurology (Minneapolis)* 1965;15:622–41.
- [6] Löfgren J, vonEssen C, Zwetnow NN. The pressure–volume curve of the cerebrospinal fluid space in dogs. *Acta Neurol Scand* 1973;49:557–74.
- [7] Marmarou A, Shulman K, LaMorgese J. Compartmental analysis of compliance and outflow resistance of the cerebrospinal fluid system. *J Neurosurg* 1975;43:523–34.
- [8] Miller JD, Garibi J, Pickard JD. Induced changes of cerebrospinal fluid volume. Effects during continuous monitoring of ventricular fluid pressure. *Arch Neurol* 1973;28:265–9.
- [9] Avezaat CJJ, van Eijndhoven JHM, deJong DA, Moolenaar WCJ. A new method of monitoring intracranial volume/pressure relationship. In: Becks JWF, Bosch DA, Brock M, editors. *Intracranial Pressure*, vol. III. Berlin: Springer-Verlag; 1976. p. 308–13.
- [10] Chopp M, Portnoy HD. Systems analysis of intracranial pressure. Comparison with volume-pressure test and CSF-pulse amplitude analysis. *J Neurosurg* 1980;53:516–27.
- [11] Hirai O, Handa H, Ishikawa M, Kim SH. Epidural pulse waveform as an indicator of intracranial pressure dynamics. *Surg Neurol* 1984;21:67–74.
- [12] Nornes H, Aaslid R, Lindegaard KF. Intracranial pulse pressure dynamics in patients with intracranial hypertension. *Acta Neurochir* 1977;38:177–86.
- [13] Szewczykowski J, Sliwka S, Kunicki A, Dytko P, Korsak-Sliwka J. A fast method of estimating the elastance of the intracranial system. A practical application in neurosurgery. *J Neurosurg* 1977;47:19–26.
- [14] Greitz D. Radiological assessment of hydrocephalus: new theories and implications for therapy. *Neurosurg Rev* 2004;27:145–65.
- [15] Foltz EL, Aine C. Diagnosis of hydrocephalus by CSF pulse-wave analysis: a clinical study. *Surg Neurol* 1981;15:283–93.



- [16] Foltz EL, Blanks JP, Yonemura K. CSF pulsatility in hydrocephalus: respiratory effect on pulse wave slope as an indicator of intracranial compliance. *Neurol Res* 1990;12:67–74.
- [17] Christensen L, Børgesen SE. Single pulse pressure wave analysis by fast Fourier transformation. *Neurol Res* 1989;11:197–200.
- [18] Contant CF, Robertson CS, Crouch J, Gopinath SP, Narayan RK, Grossman RG. Intracranial pressure waveform indices in transient and refractory intracranial hypertension. *J Neurosci Method* 1995;57:15–25.
- [19] Czosnyka M, Guazzo E, Whitehouse M, Smielewski P, Czosnyka Z, Kirkpatrick P, et al. Significance of intracranial pressure waveform analysis after head injury. *Acta Neurochir* 1996;138:531–42.
- [20] Portnoy HD, Chopp M, Branch C, Shannon MB. Cerebrospinal fluid pulse waveform as an indicator of cerebral autoregulation. *J Neurosurg* 1982;56:666–78.
- [21] Robertson CS, Narayan RK, Contant CF, Grossman RG, Gokaslan ZL, Pahwa R, et al. Clinical experience with a continuous monitor of intracranial compliance. *J Neurosurg* 1989;71:673–80.
- [22] Eide PK, Fremming AD. A new method and software for quantitative analysis of continuous intracranial pressure recordings. *Acta Neurochir* 2001;143:1237–47.
- [23] Eide PK, Due-Tønnessen B, Helseth E, Lundar T. Differences in quantitative characteristics of intracranial pressure in hydrocephalic children treated surgically or conservatively. *Ped Neurosurg* 2002;36:304–13.
- [24] Morgalla MH, Stumm F, Hesse G. A computer-based method for continuous single pulse analysis of intracranial pressure waves. *J Neurol Sci* 1999;168:90–5.
- [25] Daley ML, Gallo AE, Mauch W. Analysis of the intracranial pressure pulsation associated with the cardiac cycle. *Innov Tech Biol Med* 1986;7:537–44.
- [26] Eijndhoven JHM, van Avezaat CJJ. Cerebrospinal fluid pulse pressure and the pulsatile variation in cerebral blood volume: an experimental study in dogs. *Neurosurgery* 1986;19:507–22.
- [27] Hamer J, Alberti E, Hoyer S, Wiedemann K. Influence of systemic and cerebral vascular factors on the cerebrospinal fluid pulse waves. *J Neurosurg* 1977;46:36–45.
- [28] Wilkinson HA, Schuman N, Ruggiero J. Nonvolumetric methods of detecting impaired intracranial compliance or reactivity. Pulse width and wave form analysis. *J Neurosurg* 1979;50:758–67.
- [29] Piper IR, Chan KH, Whittle IR, Miller JD. An experimental study of cerebrovascular resistance, pressure transmission and craniospinal compliance. *Neurosurgery* 1993;32:805–16.